Ising model with conserved magnetization on the human connectome: Implications on the relation structure-function in wakefulness and anesthesia

S. Stramaglia, M. Pellicoro, L. Angelini, E. Amico, H. Aerts, J. M. Cortés, S. Laureys, and D. Marinazzo

Citation: Chaos **27**, 047407 (2017); doi: 10.1063/1.4978999
View online: http://dx.doi.org/10.1063/1.4978999
View Table of Contents: http://aip.scitation.org/toc/cha/27/4
Published by the American Institute of Physics

Ising model with conserved magnetization on the human connectome: Implications on the relation structure-function in wakefulness and anesthesia

S. Stramaglia,[1,2,3,4] M. Pellicoro,[1] L. Angelini,[1,2,3] E. Amico,[5,6] H. Aerts,[6] J. M. Cortés,[7,8] S. Laureys,[5] and D. Marinazzo[6]
[1]*Dipartimento di Fisica, Università degli Studi di Bari, Bari, Italy*
[2]*Istituto Nazionale di Fisica Nucleare, Sezione di Bari, Bari, Italy*
[3]*Center of Innovative Technologies for Signal Detection and Processing TIRES, Universit di Bari, Bari, Italy*
[4]*BCAM—The Basque Center for Applied Mathematics, Bilbao, Spain*
[5]*Coma Science Group, University of Liège, Liège, Belgium*
[6]*Faculty of Psychology and Educational Sciences, Department of Data Analysis, Ghent University, Ghent, Belgium*
[7]*Ikerbasque, The Basque Foundation for Science, E-48011 Bilbao, Spain*
[8]*Biocruces Health Research Institute, Hospital Universitario de Cruces, E-48903 Barakaldo, Spain*

(Received 28 September 2016; accepted 30 January 2017; published online 6 April 2017)

Dynamical models implemented on the large scale architecture of the human brain may shed light on how a function arises from the underlying structure. This is the case notably for simple abstract models, such as the Ising model. We compare the spin correlations of the Ising model and the empirical functional brain correlations, both at the single link level and at the modular level, and show that their match increases at the modular level in anesthesia, in line with recent results and theories. Moreover, we show that at the peak of the specific heat (the *critical state*), the spin correlations are minimally shaped by the underlying structural network, explaining how the best match between the structure and function is obtained at the onset of criticality, as previously observed. These findings confirm that brain dynamics under anesthesia shows a departure from criticality and could open the way to novel perspectives when the conserved magnetization is interpreted in terms of a homeostatic principle imposed to neural activity. *Published by AIP Publishing*. [http://dx.doi.org/10.1063/1.4978999]

It has been shown that a wide class of models, spanning a wide range from abstract to biologically detailed, reproduce large scale collective dynamics in the brain when they are in a *critical* regime. Here, we focus on possibly the simplest one, the Ising model, implemented on the structural architecture of the brain, and look at what happens when we introduce a further conservation constraint: the total magnetization remains constant at each step. We show that this leads to an improved correspondence between the structure and function at the level of modules. This phenomenon is increased in particular under loss of consciousness, when brain dynamics moves away from the critical regime, thus providing insights into how the structure and function interact in the brain.

I. INTRODUCTION

One of the key challenges in the study of complex networks is understanding the relation between the structure and the collective dynamics stemming from it. This issue is of special relevance in neuroscience, where the question translates to how structurally distinct and distant brain areas dynamically interact,[1] both in healthy and pathological conditions. Recent advances in diffusion imaging and tractography methods allow the noninvasive *in vivo* mapping of white matter cortico-cortical projections at relatively high spatial resolution,[2] yielding a connection matrix of interregional *structural connectivity* (SC). Similarly, functional MRI can be used to obtain a functional connectivity (FC) matrix, by calculating the statistical dependencies between BOLD time series measured at different sites of the brain.[3] Since the early days of *connectomics*, the relation between SC and FC has been a matter of interest, being expected but not trivial.[4,5]

The intricate interplay between the structure and function can be investigated by simulating spontaneous brain activity on structural connectivity maps. Recent studies[6–10] have implemented models of dynamical oscillators on the connectome structure.[11] These computational models vary from complex, biologically realistic spiking attractor models, describing the firing rate of populations of single neurons, over mean-field models of neuronal dynamics, down to the simple, biologically naive Ising model. All these studies agree that the best agreement of simulated functional connectivity with empirically measured functional connectivity can be retrieved when the brain network operates at the edge of dynamical instability. This state corresponds to the *critical* regime, and for the Ising model, it coincides with the maximum value of the heat capacity and of the susceptibility. In particular, some studies showed that the resting activity exhibits peculiar scaling properties, resembling the dynamics near the critical point of a second order phase transition, consistent with evidence showing that the brain at rest

is near a critical point.[12] Moreover, the possible origin and role of criticality in living adaptive and evolutionary systems have recently been ascribed to adaptive and evolutionary functional advantages.[13] In Ref. 14, the large-scale pattern of empirical brain correlations was compared with those from a large two-dimensional Ising model, showing that the match is optimal when the statistical system is close to the critical temperature. Remarkably, it has been recently argued that propofol-induced sedation and loss of consciousness move brain dynamics away from the critical regime.[15]

However, the Ising model on brain networks has so far been implemented only according to a spin dynamics in which magnetization is not preserved.[16] Another class of dynamics exists, in which the total magnetization is preserved: it is used to describe, for example, alloy systems, where the two different spin states naturally correspond to the two component atoms that comprise the alloy[17] and can be implemented via a pair exchange update rule.[18] If we consider the Ising model on the human connectome as a model of neural activity, the conservation of magnetization may be seen as a sort of homeostatic principle for the overall activity of the brain.

The question we address here is whether an Ising model with conserved magnetization on the human connectome would be a more suitable model for the functional connectivity of brain, in particular under anesthesia, where previous works have hypothesized a departure from criticality.

Under anesthesia, the brain spans a dynamical repertoire that is reduced with respect to wakefulness. This would result in an increased correspondence between structural and functional connectivity.[19,20] Following the reasoning and the results of Refs. 21 and 22, we think that this correspondence is to be sought at the level of modules rather than at the level of individual links.

II. METHODS AND DATA

A. Dynamical Ising models on brain networks

The study of the Ising model, an appealing description of phase transitions in ferromagnets, played a fundamental role in the development of the modern theory of critical phenomena (see, e.g., Ref. 23 and the recent review for Ising's model 90th birthday[24]). In the original model, a regular lattice is populated by 2-state spins, assuming one of the two values $\sigma_i = \pm 1$. Pairs of nearest neighbour spins interact so as to favour their alignment. The Hamiltonian of the system is given by

$$\mathbf{H} = -J \sum_{\langle ij \rangle} \sigma_i \sigma_j,$$

the sum being over nearest neighbour pairs on the lattice, the positive coupling J favouring ferromagnetic order. For spatial dimension $d > 1$, the model exhibits, in the thermodynamic limit, a phase transition with finite critical temperature T_c, such that above T_c the spatial arrangement of spins is disordered with an equal number of up and down spins. Below T_c, the magnetization is non-zero and distant pairs of spins are strongly correlated. All the equilibrium properties of the Ising model can be obtained from the partition function $Z = \sum exp(-\beta \mathbf{H})$, the sum being over the configurations of the system and β being the inverse temperature. Dynamical rules leading to the same equilibrium are not unique, all the possibilities being fixed by the detailed balance condition. Fundamentally, the spin dynamics may or may not conserve the total magnetization, depending on whether the Ising model is being used to describe alloy systems, where the magnetization is conserved as it is related to the composition of the material, or spin systems where magnetization is not conserved.

According to Glauber dynamics,[16] the magnetization is not conserved and each spin is sequentially considered and flipped with probability $P_{flip} = (1 + \exp(\beta \Delta E))^{-1}$, where ΔE is the energy difference associated with the spin flip. Here, we consider the Kawasaki spin-exchange dynamics,[18] which conserves the magnetization: two spins randomly chosen are swapped with probability

$$\exp(-\Delta E),$$

where ΔE is the variation of the energy corresponding to exchanging the two spins. A full iteration consists in tentatively updating all the spins (pairs of spins) for Glauber (Kawasaki) dynamics.

Turning now to couplings, let us denote A_{ij} the symmetrical structural connectivity matrix. The Hamiltonian of the Ising model on the network is

$$\mathbf{H} = -\sum_{i,j} J_{ij} \sigma_i \sigma_j,$$

where the couplings are given by $J_{ij} = \beta A_{ij}$ and the parameter β plays the role of an inverse temperature. Since we deal with finite size systems, they exhibit a (pseudo)-transition between the disordered phase and the ordered one, corresponding to the peak of the specific heat (and of the susceptibility, for the case of Glauber dynamics).

In Ref. 25, the Ising model with Glauber dynamics was implemented on the human connectome matrix of Ref. 11 at two different spatial scales, 998 and 66 nodes, and the directed and undirected information transfer between nodes was then quantified.

Spin correlations were evaluated using the classical linear Pearson correlation. The pairwise transfer entropy TE measuring the information flow from spin i to spin j in each pair connected by a link in the underlying network was computed as follows:

$$TE_{ij} = \sum_{\sigma_j = \pm 1} \sum_{\Sigma_j = \pm 1} \sum_{\Sigma_i = \pm 1} p(\sigma_j, \Sigma_j, \Sigma_i) \cdot \ldots$$
$$\ldots \cdot \log \frac{p(\sigma_j, \Sigma_j)\, p(\Sigma_j, \Sigma_i)}{p(\sigma_j, \Sigma_j, \Sigma_i)\, p(\Sigma_j)},$$

where $p(\Sigma_j, \Sigma_i)$ is the fraction of times that the configuration (Σ_j, Σ_i) is observed in the data set, and similar definitions hold for the other probabilities.

It was shown that at criticality the model displays the maximal amount of total information transfer among variables, with patterns consistent for both the coarser scale and

the denser scale. Given the fact that in this line of research we are particularly interested in information flow in networks, we have verified that the peak of the information transfer corresponds to the peak of the specific heat; therefore, a range of temperatures around the peak of the information flow (or, equivalently, the peak of the specific heat) will be taken as the critical regime of the system. It is worth mentioning that it has been observed in the regular 2D lattice Ising model that, different from the pairwise information flow which peaks at criticality, the global information transfer peaks on the disordered side of the transition, and the asymmetry observed in Ref. 26 has also been observed in Ref. 27 when considering both Ising and Kuramoto (from the viewpoint of correlations in phase synchronisation).

B. Data

The fMRI data that we consider in this work were recorded from healthy subjects in awake conditions and during propofol anesthesia. The motivation for the study, the underlying physiological issues, and the protocol are extensively described in Ref. 28. The functional MRI (fMRI) data were preprocessed with FSL (FMRIB Software Library v5.0). The first 10 volumes were discarded for correction of the magnetic saturation effect. The remaining volumes were corrected for motion, after which slice timing correction was applied to correct for temporal alignment. All voxels were spatially smoothed with a 6 mm FWHM isotropic Gaussian kernel and after intensity normalization, a band pass filter was applied between 0.01 and 0.08 Hz. In addition, linear and quadratic trends were removed. We next regressed out the motion time courses, the average CSF signal, and the average white matter signal. Global signal regression was not performed. Data were transformed to the MNI152 template, such that a given voxel had a volume of 3 mm $\times$ 3 mm $\times$ 3 mm. Finally, we obtained 116 time series, each corresponding to an anatomical region of interest (ROI), by averaging the voxel signals according to an anatomical template.[29] We selected this partition for being the most used in fMRI connectivity analysis, and because it includes subcortical structures. For the diffusion MRI data, we used the publicly available data contained in the Nathan Kline Institute- Rockland sample described and downloadable at http://fcon_1000.projects.nitrc.org/indi/pro/eNKI_RS_TRT/FrontPage.html. As a first step, the images were corrected for motion and eddy currents due to changes in the gradient field directions of the MR scanner. In particular, the eddy-correct tool from FSL was used to correct both artifacts, using an affine registration to a reference volume. After this, DTIFIT was used to perform the fitting of the diffusion tensor model for each voxel. Then, a deterministic tractography algorithm (FACT)[30] was applied using TrackVis,[31] an interactive software for fiber tracking. Two computations were performed to transform the anatomical atlas to each individual space: (1) the transformation from the MNI template to the subject's structural image (T1) and (2) the transformation from the subject's T1 to the subject's diffusion image space. Combining both transformations, each atlas region is transformed to the subject's diffusion space, allowing us to count the number of reconstructed streamlines connecting all ROI pairs.

It is worth noting that for group level analyses at the scales considered in this study, it is not relevant that the structural connectivity used for the simulations is not the one obtained from the same subjects for which the functional connectivity was computed and compared.[32]

C. Modularity and modular similarity between networks

A key concept in network theory is modularity.[33] It describes how efficiently a network can be partitioned in sub-networks, and it is particularly relevant when it comes to study the interplay between anatomical segregation and functional integration in the brain.[34] Maximization of the modularity Q allows us to identify communities. Here, we use the algorithm described in Ref. 35 which also takes into account negative weights, a situation that frequently arises in functional networks. The resolution parameter is set to its default value $\gamma = 1$ and, for each network, the algorithm was run 1000 times choosing the maximal Q and the corresponding partition. In order to compare, at the modular level, two networks with the same nodes, we calculate the similarity of their partitions quantifying it by the mutual information approach described in Ref. 36. The code used to compute these quantities is contained in the Brain Connectivity Toolbox (https://sites.google.com/site/bctnet/).

III. RESULTS

We implemented the Ising model on the structural brain networks and evaluated the transfer entropy and the spin correlations, as described in Sec. II A. The results shown here correspond to the average over 1000 runs, each consisting of 30 000 full iterations of the lattice (after discarding the transient). Since we deal with a small system, and we are not interested in the low temperature limit, we always assumed zero magnetization for Kawasaki dynamics, i.e., the starting configuration consisted of an equal number of plus and minus spins randomly assigned to nodes. In other words, due to the small size, we assume vanishing equilibrium global magnetization. We start considering, in Figure 1, the following problem: to which extent are the functional patterns of the Ising systems shaped by the underlying topology, at the level of individual links? We compare the anatomical network with the functional networks provided by the dynamical system, as a function of the inverse temperature. The following quantities are depicted, derived from the Ising model with Kawasaki dynamics on the structural connectome corresponding to awake conditions: the Pearson correlation between the transfer entropy TE and the coupling J over all the anatomically connected pairs and the Pearson correlation between spin correlations c and J over all the anatomically connected pairs. The plots of the average absolute value of the correlation and the average transfer entropy, both peaking at criticality, are also displayed for comparison. As Figure 1 shows, in the temperature regime at which information transfer and correlations are higher (identified with the critical regime, see below), the link correlation of TE and

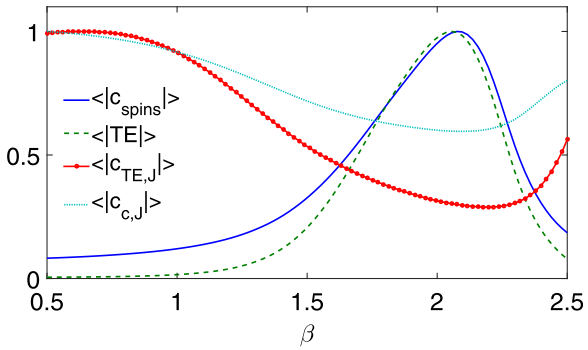

FIG. 1. The Ising model with Kawasaki dynamics is implemented on the 116 regions structural connectome. The following quantities are depicted as a function of the inverse temperature β: the correlation between the value of TE and J over all the anatomically connected pairs (red line, with bullets); the correlation between the value of c and J over all the anatomically connected pairs (cyan, dotted line); the normalized average absolute value of the correlation (blue, full line); and the normalized average transfer entropy (green, dashed line).

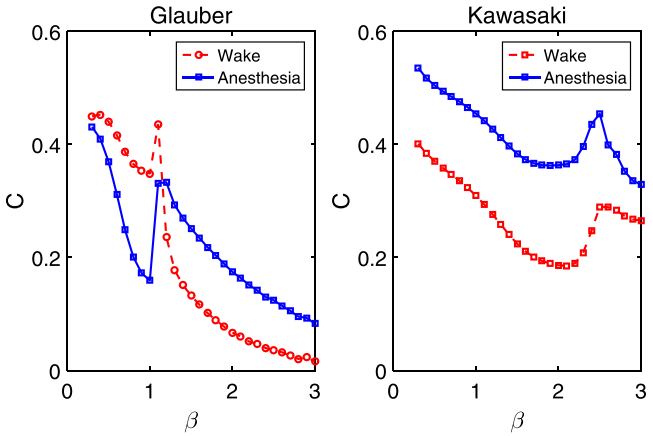

FIG. 3. The link-wise correlation between the model spin correlations and the empirical functional connectivities is depicted as a function of the inverse temperature β for wakefulness (dashed red line) and anesthesia (full blue line). Left panel: Glauber dynamics. Right panel: Kawasaki dynamics.

c, with J, is minimal; in other words, the critical states appear to be the ones at which the functional pattern is minimally shaped by the details of the underlying structural network. These findings are in line with a previous study on Ising models implemented on the connectome, in which the best fit between model and empirical correlations was observed when the entropy of the model attractors started to increase, and not at its peak.[10]

Next, in order to elucidate whether and how the fit between the model and empirical correlation changes with the level of consciousness, we consider both the fMRI data recorded from healthy subjects in awake conditions and during propofol anesthesia and the corresponding structural data. Varying the temperature, we implemented the Ising model with Kawasaki dynamics on the structural architecture connecting the 116 ROIs. We compare the corresponding spin correlations with the empirical functional correlations.

In order to visualize the typical patterns of the connectomes under examination, in Figure 2 we depict the 116 × 116 structural connectivity matrix, the empirical functional connectivity matrix for wake and anesthesia conditions, and the patterns of correlations of the Kawasaki model tuned at three different temperatures corresponding to relevant regimes in the curves described below (greatest linkwise correlation, greatest mean squared error, maximum mutual information between structural and functional modules).

As depicted in Figure 3, when the link-wise correlation between model and empirical functional patterns is considered, the match between model and empirical correlations is higher in wakefulness for Glauber dynamics, and in anesthesia for Kawasaki dynamics, in the respective critical regimes for each dynamics. Moreover, under sedation, the Kawasaki dynamics results in a better fit and in a clearer separation between wake and anesthesia, compared to the Glauber dynamics.

In Figure 4, the match between empirical and spin correlations is measured in terms of the mean square error between the two patterns, i.e., the average of $(c_{ij}^{spin} - c_{ij}^{empirical})^2$ over all pairs of brain regions, c_{ij}^{spin} being the spin correlation of the Ising models and $c_{ij}^{empirical}$ the empirical functional connectivity. Results show that again, the best match for anesthesia is better than that for wake conditions, for both Glauber and Kawasaki dynamics. Using the mean square error, however, Glauber dynamics showed a better fit.

However, it has been shown that a modular comparison is better suited to investigate the interplay between the structure

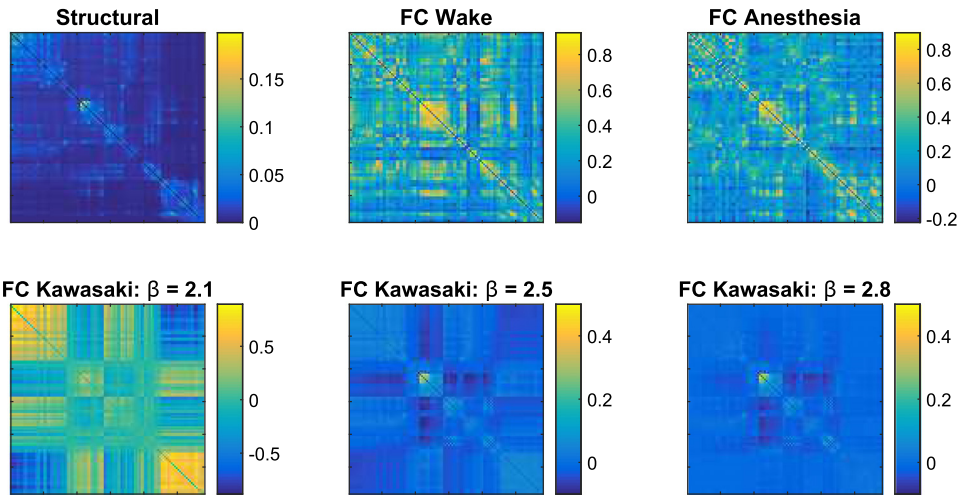

FIG. 2. Top: matrices corresponding to empirical data. Structural connections (left), average correlations in wakefulness (center), and average correlations in anesthesia (right). Bottom: average correlations in simulated time series for three values of the inverse temperatures, corresponding to relevant points in the curves of the following figures.

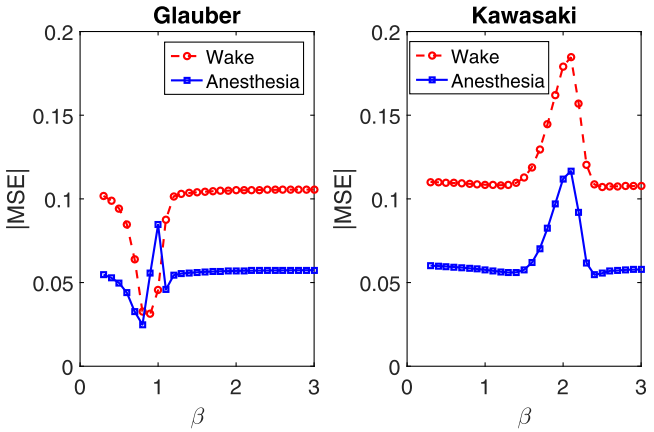

FIG. 4. The mean square error between the model spin correlations and the empirical functional connectivities is depicted as a function of the inverse temperature β for wakefulness (dashed red line) and anesthesia (full blue line). Left panel: Glauber dynamics. Right panel: Kawasaki dynamics.

and function.[21] Hence, in order to better describe the relation between empirical and simulated functional patterns at the modular level, we have evaluated the mutual information between partitions (obtained by maximizing the modularity) as a function of β to quantify the relation between empirical functional correlations and spin correlations from the model, for wake subjects and subjects under anesthesia. In Figure 5, the mutual information is plotted for both Kawasaki and Glauber dynamics. In wakefulness, where the same structural connectivity subserves a wide repertoire of activity, we observe a reduction of the mutual information in the critical regime with respect to the disordered phase, for both Glauber and Kawasaki dynamics. This behavior is reversed, leading to increased mutual information between structural and functional models, for the Kawasaki dynamics under sedation.

These results speak to the fact that Ising models tuned at criticality result in connectivity matrices with a generally good linkwise resemblance with the empirical ones, comparable or even better than the one obtained with more biologically precise models.[37,38] This similarity is represented by a peak in the curves in Figure 3 which follows a trough,

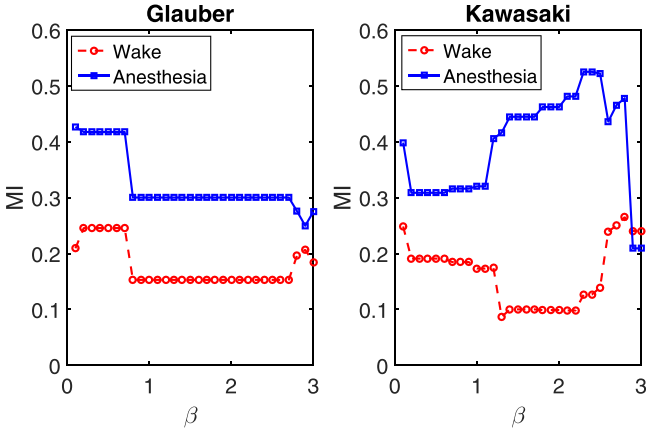

FIG. 5. The mutual information between the partitions of the empirical and model functional networks, as a function of the inverse temperature β is depicted for Kawasaki and Glauber dynamics, and for wake and anesthesia conditions. The modular decomposition is obtained by maximization of modularity.

corresponding to the peak in mean squared error of 4. According to the pairwise metric though, the best resemblance remains the not-so-interesting one corresponding to the limit of high temperatures. On the other hand, if we look at the mutual information between structural and functional modules, we can observe that, with respect to the disordered phase, Kawasaki dynamics in the critical regime leads to a decreased match between structural and functional modules in wakefulness, and an increased one in anesthesia. These results, in line with our hypotheses, are not evidenced by Glauber dynamics.

IV. DISCUSSION AND CONCLUSIONS

We have considered pair exchange update rules for the Ising model[18] implemented on the structural brain network at the macroscale, using a data set of healthy subjects scanned during quiet wakefulness and during deep sedation, a condition in which the structure-function relation is modified. Our results show that the structure-function relation is strengthened under anesthesia, both at the link and modular levels, compared to wake conditions. Having shown that at criticality the functional pattern is less dependent on the underlying structural network, it follows that anesthesia takes the brain dynamics farther from the critical regime, in accordance with previous evidence.

Moreover, at the modular level we obtained a better match with empirical functional correlations using Kawasaki dynamics compared to the more common Glauber dynamics for which the magnetization is not preserved.[16] This improved match suggests that the conservation law of the Kawasaki dynamics might admit a physiological counterpart. A possible interpretation is seeing it as an *effective* implementation, due to the time scale separation, of the coupling from metabolic resources to neural activity, a key ingredient that is missing in neural models on the connectome.[39]

In agreement with recent theoretical frameworks,[40] our results suggest that a wide range of temperatures correspond to *criticality* of the dynamical Ising system on the connectome, rather than a narrow interval centered in a critical state. In such critical conditions, the correlational pattern is minimally shaped by the underlying structural network. It follows that, assuming that the human brain operates close to a *critical* regime,[41] there is an intrinsic limitation in the relationship between the structure and function that can be observed in data. We have shown that empirical correlations among brain areas are better reproduced at the modular level using a model which conserves the global magnetization. The most suitable way to compare functional and structural patterns is to contrast them at the network level, using, e.g., the mutual information between partitions like in the present work.

During the awake resting state, spontaneous brain activity constantly fluctuates across brain regions, exhibiting a rich repertoire of functional connectivity patterns. Previous studies accounted for long-range resting-state functional connectivity persisting even after loss of consciousness.[42–44] A recent study on monkeys[19] posited that the role of structural connectivity in sculpting functional connectivity maps

changes during wakefulness and anesthesia. According to the authors, wakefulness seems to be characterized by a rich repertoire of connectivity patterns, while the functional connectivity patterns under sedation follow the underlying brain structure. Another study reports increased similarity between whole-brain anatomical and functional connectivity networks during deep sleep.[20] Our results, showing that the structure-function correspondence is enhanced under anesthesia at the modular level, are in accordance with this evidence.

Summarizing, we have considered the Ising model as a valuable tool to explore large scale brain dynamics. We have shown that the conservation of magnetization leads to better correspondence between the structure and function, notably where this is more expected, that is in loss of consciousness, again speaking to a less critical dynamical regime. The reason of this improvement might lie in the features added by the Kawasaki dynamics to large scale connectivity (i.e., negative correlations). Its biological counterparts could be intuitively found in some homeostasis mechanism or metabolic constraint, but no validation tools for this conjecture exist at the moment.

Finally, our results confirm that matches between the structure and function should be sought at the modular level rather than among individual links, in line with recent work.[21,22,45]

[1]H.-J. Park and K. Friston, Science **342**, 1238411 (2013).
[2]O. Sporns, *Networks of the Brain* (Cambridge, MA, 2011), p. 412.
[3]H. H. Shen, Proc. Natl. Acad. Sci. **112**, 14115 (2015).
[4]M. P. van den Heuvel, R. C. W. Mandl, R. S. Kahn, and H. E. Hulshoff Pol, Human Brain Mapp. **30**, 3127 (2009).
[5]A. M. Hermundstad, D. S. Bassett, K. S. Brown, E. M. Aminoff, D. Clewett, S. Freeman, A. Frithsen, A. Johnson, C. M. Tipper, M. B. Miller, S. T. Grafton, and J. M. Carlson, Proc. Natl. Acad. Sci. U. S. A. **110**, 6169 (2013).
[6]C. J. Honey, O. Sporns, L. Cammoun, X. Gigandet, J. P. Thiran, R. Meuli, and P. Hagmann, Proc. Natl. Acad. Sci. U. S. A. **106**, 2035 (2009).
[7]J. Cabral, E. Hugues, O. Sporns, and G. Deco, NeuroImage **57**, 130 (2011).
[8]G. Deco, V. K. Jirsa, and A. R. McIntosh, Nat. Rev. Neurosci. **12**, 43 (2011).
[9]G. Deco and V. K. Jirsa, J. Neurosci. **32**, 3366 (2012).
[10]G. Deco, M. Senden, and V. Jirsa, Front. Comput. Neurosci. **6**, 68 (2012).
[11]P. Hagmann, L. Cammoun, X. Gigandet, R. Meuli, C. J. Honey, V. J. Wedeen, and O. Sporns, PLoS Biol. **6**, e159 (2008).
[12]A. Haimovici, E. Tagliazucchi, P. Balenzuela, and D. R. Chialvo, Phys. Rev. Lett. **110**, 178101 (2013); e-print arXiv:1209.5353.
[13]J. Hidalgo, J. Grilli, S. Suweis, M. A. Muñoz, J. R. Banavar, and A. Maritan, Proc. Natl. Acad. Sci. U. S. A. **111**, 10095 (2014).
[14]D. Fraiman, P. Balenzuela, J. Foss, and D. R. Chialvo, Phys. Rev. E: Stat. Nonlinear Soft Matter Phys. **79**, 061922 (2009).
[15]E. Tagliazucchi, D. R. Chialvo, M. Siniatchkin, E. Amico, J.-F. Brichant, V. Bonhomme, Q. Noirhomme, H. Laufs, and S. Laureys, J. R. Soc. Interface **13**, 20151027 (2016).
[16]R. J. Glauber, J. Math. Phys. **4**, 294 (1963).
[17]P. L. Krapivsky, S. Redner, and E. Ben-Naim, *A Kinetic View of Statistical Physics* (Cambridge University Press, 2010), Vol. 18.
[18]K. Kawasaki, Phys. Rev. **145**, 224 (1966).
[19]P. Barttfeld, L. Uhrig, J. D. Sitt, M. Sigman, B. Jarraya, and S. Dehaene, Proc. Natl. Acad. Sci. **112**, 887 (2015).
[20]E. Tagliazucchi, N. Crossley, E. T. Bullmore, and H. Laufs, Brain Struct. Funct. **221**, 4221 (2016).
[21]I. Diez, P. Bonifazi, I. Escudero, B. Mateos, M. A. Muñoz, S. Stramaglia, and J. M. Cortes, Sci. Rep. **5**, 10532 (2015).
[22]B. Mišić, R. F. Betzel, M. A. de Reus, M. P. van den Heuvel, M. G. Berman, A. R. McIntosh, and O. Sporns, Cereb. Cortex **26**, 3285 (2016).
[23]K. Huang, *Statistical Mechanics* (Wiley, 1987), p. 493.
[24]A. Taroni, Nat. Phys. **11**, 997 (2015).
[25]D. Marinazzo, M. Pellicoro, G. Wu, L. Angelini, J. M. Cortés, and S. Stramaglia, PLoS ONE **9**, e93616 (2014).
[26]L. Barnett, J. T. Lizier, M. Harré, A. K. Seth, and T. Bossomaier, Phys. Rev. Lett. **111**, 177203 (2013).
[27]M. Botcharova, S. F. Farmer, and L. Berthouze, Front. Syst. Neurosci. **8**, 176 (2014).
[28]P. Boveroux, A. Vanhaudenhuyse, M.-A. Bruno, Q. Noirhomme, S. Lauwick, A. Luxen, C. Degueldre, A. Plenevaux, C. Schnakers, C. Phillips, J.-F. Brichant, V. Bonhomme, P. Maquet, M. D. Greicius, S. Laureys, and M. Boly, Anesthesiology **113**, 1038 (2010).
[29]N. Tzourio-Mazoyer, B. Landeau, D. Papathanassiou, F. Crivello, O. Etard, N. Delcroix, B. Mazoyer, and M. Joliot, NeuroImage **15**, 273 (2002).
[30]S. Mori, B. J. Crain, V. P. Chacko, and P. C. van Zijl, Ann. Neurol. **45**, 265 (1999).
[31]R. Wang, T. Benner, a. G. Sorensen, and V. J. Wedeen, Proc. Int. Soc. Magn. Reson. Med. **15**, 3720 (2007).
[32]P. Sanz Leon, S. A. Knock, M. M. Woodman, L. Domide, J. Mersmann, A. R. McIntosh, and V. Jirsa, Front. Neuroinf. **7**, 10 (2013).
[33]M. E. J. Newman, Proc. Natl. Acad. Sci. **103**, 8577 (2006).
[34]O. Sporns and R. F. Betzel, Annu. Rev. Psychol. **67**, 613 (2016).
[35]M. Rubinov and O. Sporns, NeuroImage **56**, 2068 (2011).
[36]M. Meil, J. Multivar. Anal. **98**, 873 (2007).
[37]G. Deco, A. Ponce-Alvarez, D. Mantini, G. L. Romani, P. Hagmann, and M. Corbetta, J. Neurosci. **33**, 11239 (2013).
[38]M. I. Falcon, J. D. Riley, V. Jirsa, A. R. McIntosh, A. D. Shereen, E. E. Chen, and A. Solodkin, Front. Neurol. **6**, 228 (2015).
[39]J. A. Roberts, K. K. Iyer, S. Vanhatalo, and M. Breakspear, Front. Syst. Neurosci. **8**, 154 (2014).
[40]P. Moretti and M. a. Muñoz, Nat. Commun. **4**, 2521 (2013); e-print arXiv:arXiv:1308.6661v1.
[41]D. R. Chialvo, Nat. Phys. **6**, 744 (2010).
[42]J. L. Vincent, G. H. Patel, M. D. Fox, A. Z. Snyder, J. T. Baker, D. C. Van Essen, J. M. Zempel, L. H. Snyder, M. Corbetta, and M. E. Raichle, Nature **447**, 83 (2007).
[43]D. Fernández-Espejo, A. Soddu, D. Cruse, E. M. Palacios, C. Junque, A. Vanhaudenhuyse, E. Rivas, V. Newcombe, D. K. Menon, J. D. Pickard, S. Laureys, and A. M. Owen, Ann. Neurol. **72**, 335 (2012).
[44]P. Guldenmund, A. Vanhaudenhuyse, M. Boly, S. Laureys, and A. Soddu, Arch. Ital. Biol. **150**, 107 (2012).
[45]R. Kujala, E. Glerean, R. K. Pan, I. P. Jääskeläinen, M. Sams, and J. Saramäki, Eur. J. Neurosci. **44**, 2673 (2016).